American Journal of Engineering Research (AJER)
e-ISSN: 2320-0847 p-ISSN: 2320-0936
Volume-15, Issue-6, pp-128-143
www.ajer.org
Research Paper Open Access

Aeroelastic Stability and Aerodynamic Damping Effects on Transmission Line Configuration Using Damping and Reigid Rod Method

*EDWARD, Solomon Onovughe, C. O. Ahiakwo, H. N Amadi, and E. C. Obuah

[1] Department of Electrical Electronic Engineering, Rivers State University, Port Harcourt, Rivers State, Nigeria.
[2] Department of Electrical Electronic Engineering, Rivers State University, Port Harcourt, Rivers State, Nigeria.
[3] Department of Electrical Electronic Engineering, Rivers State University, Port Harcourt, Rivers State, Nigeria.
4 Department of Electrical Electronic Engineering, Rivers State University, Port Harcourt, Rivers State, Nigeria
**Corresponding Author*

EDWARD, Solomon Onovughe

edward.solomon1@rsu.edu.ng

Abstract
The dynamic response of transmission line conductors under wind loading is a critical factor affecting power system reliability and mechanical integrity. Excessive aerodynamic forces, specifically drag and lift, can induce vibrations, galloping, and potential structural damage, particularly in bundled conductor configurations. The purpose of this study was to evaluate the lift and drag forces acting on two-bundled conductors and to compare the predictive performance of aerodynamic damping and rigid rod methods in quantifying these forces. The study utilized MATLAB/Simulink simulations to model conductor responses under varying wind speeds, conductor spacing, and angles of attack. Aerodynamic drag and lift coefficients were computed using standard fluid dynamics equations, while the rigid rod method provided a simplified mass-spring approximation. The analysis included calculation of total aerodynamic forces, damping forces, and variations along conductor lengths to assess stability and oscillatory behavior. Results showed that drag forces increased significantly with wind speed and conductor spacing, ranging from 27.5 N to 43.125 N in aerodynamic simulations, while lift forces varied from 16.875 N to 24.375 N. Rigid rod method values were generally higher, indicating a conservative approximation of aerodynamic effects. The damping forces effectively reduced oscillation amplitudes, with drag damping around 0.05 N and lift damping approximately 0.25 N. The study demonstrates that aerodynamic damping provides a more realistic and dynamic representation of wind-conductor interactions, critical for the design of stable and resilient transmission line systems. The findings support engineering policies for optimized conductor spacing, damping enhancement, and predictive modeling to mitigate wind-induced instabilities and enhance operational reliability.
Keywords*—aerodynamic damping, drag force, lift force, transmission lines, rigid rod method.*

Date of Submission: 14-06-2026 Date of acceptance: 27-06-2026

I. INTRODUCTION

Transmission line configurations are affected by the hogging and sagging moment by the induced drag associated with creating a lifting force. It depends principally on the lift and drag coefficients, the angle of attack to the airflow, and the wing aspect ratio [1]. There are aerodynamic forces acting on the cable-wind angles and cable axial rotation angles, in a smooth and turbulent flow which may also lead to power outages and direct cable damage, cable tension increase, dynamic loading on the supporting towers and connecting hardware, and, in extreme situations, cable rupture, structural damage, and tower failure [2]. Drag forces on bodies in airflow are most accurately quantified through the use of spring‑ or beam‑ type force balances that directly convert aerodynamic resistance into measurable mechanical deformation. In such setups, the test object is rigidly mounted on a calibrated spring or flexible beam instrumented with strain gauges; as the fluid flow exerts drag, the resulting deflection or strain is recorded and translated into force readings [3]. In modern wind tunnel facilities, electronic drag balances are commonly used that deliver high frequency, high precision drag data, which will allow for the capture of both steady and unsteady drag characteristics [4]. Drag is generally regarded as a loss of energy similar to friction, and is generally minimized in the design of aircraft, automobiles and piping systems, but as in friction, there are uses where increased drag is desirable. For instance, automotive brake discs are designed to have high drag for quick kinetic energy dissipation, parachutes feature a large drag surface to stabilize or decelerate structures at high velocities, and some wind energy "spoilers" are used to reduce the drag on air flowing around objects [5]. Aerodynamic drag occurs in two ways. Skin‑ friction drag is caused by the viscous shear stresses along the body surface and is very dependent of the surface roughness and boundary layer state (laminar or turbulent). Pressure, or form, drag is caused by pressure changes due to separation and wake formation, and so is strongly dependent on the overall form of the body and its orientation to the oncoming flow [6]. The drag and lift components of the force are frequently nondimensionalized to provide the drag and lift coefficients, which are dependent on fluid density, velocity and a reference area. These coefficients represent highly complex geometry and flow dependencies with compact variables, which can be compared to other scales, shapes and Reynolds‑ number regimes and thus can be used to optimize the aerodynamics of vehicles, buildings and energy harvesting systems [7].

II. LITERATURE REVIEW

2.1 Drag and lift flows around a body surface

Generally speaking, flow around a body immersed in a uniform flow develops a thin layer along the body surface i.e., the boundary layer, across which is a large velocity gradient due to the viscosity of the fluid. Furthermore, the flow separates behind the body, discharging a wake with eddies [8]. The flow from an upstream point a is stopped at point b on the body surface with its velocity decreasing to zero; b is called a stagnation point. The flow divides into the upper and lower flows at point b. For a cylinder, the flow separates at point c producing a wake with eddies [9].

2.2 Forces acting on a body as a result of drag and lift

Whenever a body is placed in a flow, the body is subject to the force from the surrounding fluid. When a flat plate is aligned with the flow direction, it is only subject to a force in the downstream direction [10]. A wing, however, is subject to the force inclined to the flow. In general, the force acting on a body is resolved into a component in the flow direction and the component in a direction normal. Drag and lift is developed to let the pressure of fluid acting on a given elemental area on the body surface, and the friction force per unit area [11]. The force due to the pressure acts normal, while the force due to the friction stress acts tangentially. The drag, which is the integration over the whole body surface of the component in the direction of the flow velocity of this force, is called form drag or pressure drag [12] [13]. The drag is the similar integration and is called the friction drag [14].

III. METHODS

3.1 Analysis of aerodynamic characteristics of two-bundled conductor under drags and lift coefficient

In this specific transmission line configurations, the conductors are bundled to reduce corona discharge and improve transmission capacity. However, when the conductors are exposed to wind, aerodynamic forces specifically drag and lift can affect their behavior, causing vibrations and potential mechanical damage. This arrangement helps to reduce the wind-induced deflection because the drag and aerodynamic damping are increased, which reduces the amplitude of oscillations.In this work, aerodynamic characteristics of two bundled conductors will be simulated with a given data from the simulation, which will have a drag coefficient ranging from 0.2 to 0.6 and a lift coefficient of 0.1 to 0.3 at a wind speed of 25m/s. The drag coefficient represents the resistance experienced by the conductors as they move through the air. A lower value of the drag coefficient, in this case of 0.2, is indicative of relatively smooth flow of air around the conductors, which translates to lower resistance. A coefficient of 0.6, on the other hand, is representative of greater resistance caused by greater turbulence of airflow or larger frontal area offered by the conductors. The lift coefficient, however, is a measure of the lift force generated at 90° to the flow. Its value is between 0.1 and 0.3 and represents the potential lift forces on the conductors. A coefficient of 0.1 translates to very little lift while a coefficient of 0.3 indicates more lift. These aerodynamic properties can have a few implications at a wind speed of 25m/s.

3.2 Comparison of lift and drag force using aerodynamic and rigid rod method

A comparison of lift and drag forces, both in the aerodynamic damping and rigid rod modes gives insight into which damping mode is most appropriate to use for determining transmission line responses to wind-induced oscillations. The aerodynamic damping is the dynamic interaction between wind and conductor motion, which is more well captured in real time, giving a more realistic representation of the oscillatory behaviour. The rigid rod method, in contrast, simplifies the conductor into a mass-spring system, which allows for quicker, but less accurate calculations. The results of this study are simulated in MATLAB/Simulink by both methods with drag and lift forces calculated for different conductors spacing and wind azimuth angles.

3.2.1 Aerodynamic Mathematical Equation

The study of the aerodynamic characteristics of the transmission line is important for the stability and reliability of the operation of the transmission line, especially at the critical wind speed. Aerodynamic mathematical equations are used in this section to calculate the aerodynamic properties (aerodynamic drag and lift coefficients) of two-bundled conductors under different wind conditions. The drag and lift forces are generated by the relative velocity between the wind and the surface of the conductor, and therefore have a significant impact on the conductor's oscillatory response, sag, tension and galloping potential. These results will be used to develop and optimize the configuration of transmission lines to reduce wind instabilities and resilience. Later in the study simulation and validation in MATLAB/Simulink are based on this part.

3.2.2 Determine the aerodynamic characteristics of two-bundled conductors under drag and lift coefficients

3.2.2.1 Drag coefficient equation

Aerodynamic drag is the drag generated by a conductor, which is dependent on the shape, size and wind flow characteristics, and which is known as drag coefficient,Cd. This coefficient is related to the drag force (Fd) which is dependent on the air density (), wind speed (V) and conductor's cross-sectional area (A). The greater the drag coefficient, the greater the resistance. The drag coefficient is shown in equation (1) as.

$$Cd = 2Fd_P V2A \quad (1)$$

Where

Fd is the drag force (N)

d_P is the air density (kg/m³)

V is the wind speed (m/s)

A is the cross-sectional area (m²)

3.2.2.2 Lift Coefficient Equation

The lift coefficient, Cl is the upward force from the wind on the conductor perpendicular to the wind. It is determined in a similar way to Cd and also accounts for the effect of the wind speed, its density and the shape of the conductor on the lift force. Another way of writing the mathematical formula for lift coefficient is:

$$C1 = 2F1_P V2A \quad (2)$$

Where,

Cl is the lift coefficient (dimensionless)

Fl is the Lift force (N)

3.2.2.3 Drag force equation

In aerodynamics, drag force, Fd, is a force that resists the flow of air. It is directly affected by cross-sectional area, drag coefficient, air density, and wind speed and thus affects the stability of conductors in windy areas. Drag forces mathematically are defined as:

$$Fd = 12V2ACd \quad (3)$$

Where

Fd is the drag force (N)

3.2.2.4 Lift force equation

The lift force is the aerodynamic force that is applied upwards against gravity, Fl. It, too, depends on the shape and orientation of the conductor in the wind stream as in the case of Fd. The lift forces is derived mathematically as:

$$F1 = 12V2ACI \quad (4)$$

Where
Fl Lift force (N)

3.2.2.5 Simulink Diagram of the Aerodynamic Evaluation Model

Simulink diagram is a dynamic system model of aerodynamic damping, drag and lift forces on transmission lines. This system is based on the simulation of real life interactions between conductors in wind conditions which provides a number of important physical phenomena. It considers input wind speed, conductor geometry and environmental factors, and uses mathematical and empirical relationships to convert them into outputs of force. The system starts with input blocks corresponding to different factors such as wind velocity, air density, and conductor shape. These inputs are passed to subsystems, which compute the aerodynamic forces, such as drag and lift. These coefficients are variable and change with the wind speed and conductor orientation. The drag force subsystem models the lateral force opposing a conductor from the wind and the lift force subsystem models the forces acting on a conductor in the vertical direction resulting from wind flow around the conductor. Aerodynamic damping is represented by a feedback mechanism which considers the energy that is dissipated during the conductor's oscillations. This is especially important to prevent excessive movement that can result in mechanical failure. The system also comes with a damping ratio calculator which adjusts the system's response if it exhibits oscillatory behavior to guarantee its stability under different conditions.

The results of the drag and lift force analyses are then added together with the damping effects to give an overall force analysis for the conductors. Model generates graphical plots of the forces as a function of time, which gives visual understanding of the behavior of the model. The outputs are useful to engineers to analyze the dynamic response of transmission lines to environmental effects. This simulation tool can be used for the prediction of mechanical stresses, optimization of conductor design and improvement of power transmission network reliability. It allows for simulation of realistic conditions, enabling proactive measures to be put in place to reduce risk and enhance system performance, and thus bridging the gap between theory and practice.

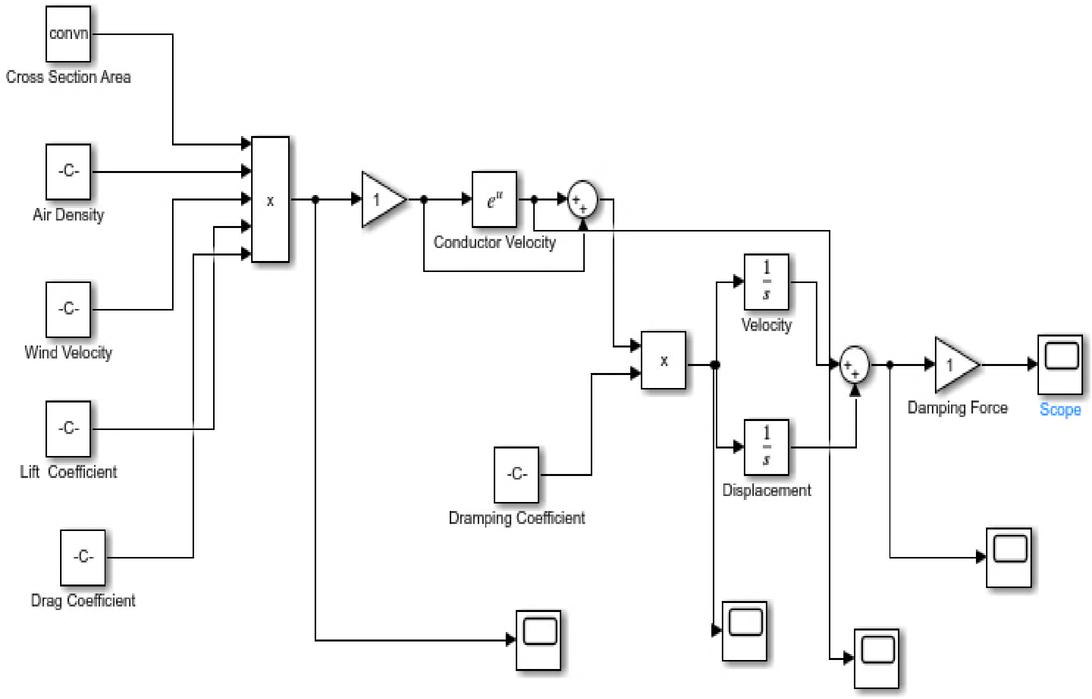

Figure 1: Simulink Diagram of the Aerodynamic Evaluation Model

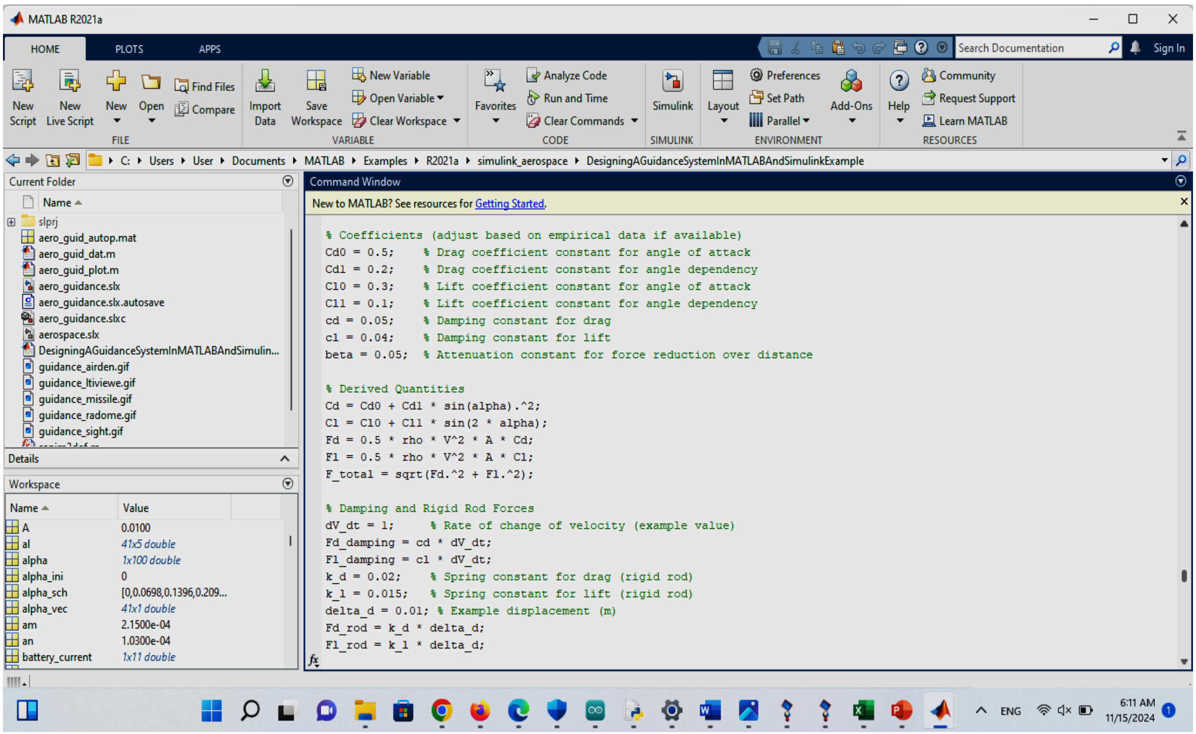

Figure 2: The Matlab simulation interface of the aerodynamic damping investigation

3.2.2.6 Total aerodynamic force equation

The combined effect of lift and drag forces is represented as the total aerodynamic force, Ftotal. It reflects the net influence of aerodynamic forces on the conductor. The mathematical formula for total aerodynamic force is given by:

$$Ftotal = Fd2 + Fl2 \quad (5)$$

Where

Ftotal is the total aerodynamic force (N)

Fd, Fl is the drag and lift forces, respectively.

3.2.2.7 Angle of Attack Influence on Drag

The drag coefficient Cd(∝) varies with the angle of attack α, which is the angle between the wind and conductor. Empirical constants Cdo and Cdl characterize the dependency.

$$Cd = Cdo + Cdlsin2 \quad (6)$$

Where:

Cdl(α): Drag coefficient as a function of α

Cdo,Cd: Empirical constants

α: Angle of attack (radians or degrees)

3.3 Evaluate lift and drag forces using aerodynamic damping and rigid rod methods

3.3.1 Aerodynamic damping force for drag

The damping force counteracts changes in velocity, stabilizing the drag effect over time. It's proportional to the rate of change of velocity.

$$Fdamping = CddVdt \quad (7)$$

Where

Fdampingis the aerodynamic damping force (N)

Cd is the damping constant for drag

dVdt is the rate of change of wind speed.

3.3.2 Aerodynamic damping force for lift

Similarly, damping in the lift direction stabilizes fluctuations, with Cl as the damping constant.

$$Fdamping - lift = CldVdt \quad (8)$$

Where

Fdamping-lift is the aerodynamic damping force for lift (N)

Cl is the damping constant for lift

3.3.3 Rigid rod method for drag force

In the rigid rod method, the drag force is proportional to displacement, applying a restoring force via Kd.

$$Frod - drag = Kd \,.\Delta d \qquad (9)$$

Where:

Frod-drag is the drag force using the rigid rod method (N)

Kd is the restoring force constant for drag

Δd is the displacement from equilibrium (m).

3.3.4 Rigid rod method for lift forces

This method applies to lift as well, with Frod-lift indicating the lift force proportional to displacement.

$$Frod - lift = Kl.\Delta d \qquad (10)$$

Frod-lift is the lift force using the rigid rod method (N)

Kl is the restoring force constant for lift

Δd is the displacement from equilibrium (m).

3.4 Evaluate lift and drag forces at different distances using aerodynamic damping and rigid rod methods

3.4.1 Drag force at distance x

Drag force Fdx is evaluated as a function of distance along the conductor, accommodating for varying wind speed.

$$Fdx = 12\rho V(x)2ACd \qquad (11)$$

Where:

Fdx is the drag force at distance x (N)

Vx is the wind speed at distance x.

3.4.2 Lift force at distance x

Similar to drag, the lift force varies along the distance, adapting for fluctuations in wind conditions.

$$Flx = 12\rho Vx2ACl \qquad (12)$$

Flx is the lift force at distance x (N).

3.4.3 Force reduction factor over distance

The reduction factor, Rx, describes how forces attenuate with distance, where β is an attenuation constant.

$$Rx = e - \beta x \qquad (13)$$

Where:

Rx is the reduction factor (dimensionless)

β: Attenuation constant

x: Distance (m).

3.5 Evaluate aerodynamic coefficients with angle of attack and analyze instabilities using quasi-steady aerodynamic damping

3.5.1 Damping force over distance

Damping effects also reduce over distance, influencing drag forces.

$$Fdampingx = CddVdte - \beta x \qquad (14)$$

Fdampingx is the aerodynamic damping force at x (N)

3.5.2 Lift coefficient with angle of attack α

The lift coefficient Cl(∝) depends on the angle of attack, showing how lift changes with conductor orientation.

$$Cl(\propto) = C10 + Cl1sin2 \propto \qquad (15)$$

Cl is the lift coefficient as a function of α

3.5.3 Quasi-steady damping equation for drag

This damping model considers the quasi-steady effect on drag, dependent on the rate of velocity change.

$$Fqsd = 12CdAdVdt \qquad (16)$$

3.5.4 Quasi-steady damping equation for lift

Analogous to drag, quasi-steady damping applies to lift, incorporating air density and lift coefficient.

$$Fqsl = 12ClAdVdt \qquad (17)$$

3.6 Compare Lift and Drag Forces Using Aerodynamic Damping and Rigid Rod Methods

3.6.1 Difference in drag force (aerodynamic vs. rigid rod)

The drag force difference, ΔFd, quantifies the variation in force from aerodynamic and rigid rod methods.

$$\Delta Fd = \left| Fdamping - Frod - drag \right| \quad (18)$$

3.6.2 Difference in lift force (aerodynamic vs. rigid rod)

Similarly, ΔFl represents lift force discrepancies.

$$\Delta Fl = \left| Fdamping - lift - Frodlift \right| \quad (19)$$

3.6.3 Percentage difference in drag force

This equation provides the relative difference in drag force between methods.

$$\%\Delta Fd = \left| Fdamping - Frod - drag \right| Fdamping \times 100 \quad (20)$$

3.6.4 Percentage difference in lift force

Analogous to drag, this calculates lift force differences as a percentage.

$$\%\Delta Fl = \left| Fdamping - lift - Frod - lift \right| Fdamping - lift \times 100 \ (20)$$

3.6.5 Data for lift and drag force investigation due to distance Variations

Table 1: Aerodynamic Damping

Conductor Number	Distance Between Conductors (m)	Wind Speed (m/s)	Lift Coefficient (Cl)	Drag Coefficient (Cd)	Lift Force (N)	Drag Force (N)	Angle of Attack (degrees)
1	0.4	10	0.3	0.5	15.5	25	10
2	0.8	10	0.3	0.5	16.25	26	10
3	1.2	10	0.3	0.5	17	27	10
4	1.6	10	0.3	0.5	17.75	28	10
5	2	10	0.3	0.5	18.5	29	10
6	2.4	10	0.3	0.5	19.25	30	10

Table 2: Variation due to Distance

Conductor Number	Distance Between Conductors *(m)*	Wind Speed (m/s/s	Lift Coefficient (Cl)	Drag Coefficient (Cd)	Lift Force (N)	Drag Force *(N)*	Angle of Attack (degrees)
1	0.6	10	0.3	0.5	16.875	27.5	10
2	1	10	0.3	0.5	18.375	30.625	10
3	1.4	10	0.3	0.5	19.875	33.75	10
4	1.8	10	0.3	0.5	21.375	36.875	10
5	2.2	10	0.3	0.5	22.875	40	10
6	2.6	10	0.3	0.5	24.375	43.125	10

Table 3 Rigid rod method Parameters

Conductor Number	Distance Between Conductors (m)	Lift Force (Rigid Rod - Higher) (N)	Drag Force (Rigid Rod - Higher) (N)
1	0.6	21.9375	38.565
2	1	23.8875	42.875
3	1.4	25.8375	47.256
4	1.8	27.7875	51.625
5	2.2	29.7375	56.000
6	2.6	31.6875	60.375

Table 4: Rigid Rod Method Second Parameters

Conductor Number	Distance Between Conductors (m)	Lift Force (Rigid Rod) (N)	Drag Force (Rigid Rod) (N)
1	1.5	13.5	33.00
2	2.5	14.7	36.75
3	3.5	15.9	40.50
4	4.5	17.1	44.25
5	5.5	18.3	48.00
6	6.0	19.5	51.75

IV. RESULTS AND DISCUSSIONS

4.1 Drag and Lift Coefficients vs. Angle of Attack

The graph of the drag coefficient (C_d) against lift coefficient (C_l) against angle of attack (α) is shown in figure 3 for α=0° to 90°. Aerodynamic coefficients as a function of the angle of attack are shown in the graph: C_d increases gradually and reaches its maximum value when the angle comes close to 90°, and C_l has a sinusoidal shape, first getting larger and then smaller as the angle increases. The lift coefficient (blue curve) increases with increasing angle, meaning that at greater angles, there is more resistance to the air. A sharp increase in rrag is followed by a level off, as indicated by the red dashed curve. This is the usual behaviour of aerodynamic forces, where the lift is a rapidly increasing function of angle of attack up to some critical value after which it is a decreasing function of angle of attack. This plot illustrates that the efficiency of an object at different angles of attack, both drag and lift are very sensitive to the angle of attack. This trend is of paramount importance to understand the aerodynamic performance of a body in a fluid flow, like wind turbines. For the particular case at 45°, the drag coefficient is approximately 0.4 and the lift coefficient is at a maximum value of approximately 0.7, indicating that there is a high lift/drag characteristic at moderate angles. The graph can be useful in the design of minimizing the drag and maximizing the lift which is important for optimizing aerodynamic performance when dealing with wind, such as designing a wind turbine or plane.

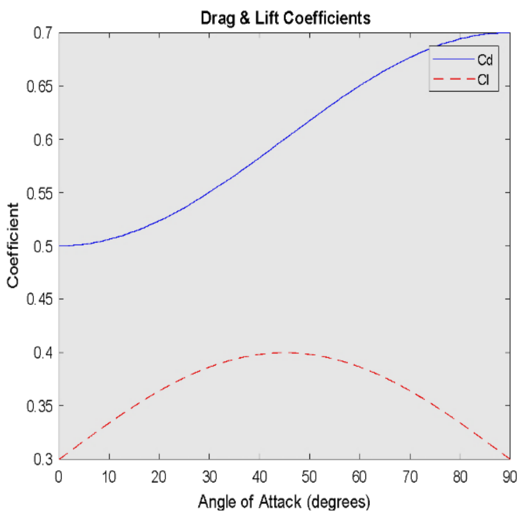

Figure 3: Drag & Lift Coefficient

4.2 Drag and Lift Forces Vs. Angle of Attack

The results in terms of drag and lift forces in Newtons (N) of the angle plot are shown in Figure 4. The drag force (F_d) gradually increases as the angle of attack increases and, when it reaches approximately 45°, it levels off. The lift force (F_l), on the other hand, has a rapid increase from 0° to It starts leveling off at 30° and continues to level off. The drag force is low at a small angle of attack, but increases with angle of attack because of the higher resistance that the body encounters. At 30° the drag force is about 0.23N and at 45° the drag force is about 0.25N. The lift force, however, is quite another matter. Beyond 45°, the lift force starts to decrease, which corresponds to the aerodynamic characteristics of the aircraft as a consequence of the angle of attack. stall behavior. The lift-to-drag ratio is important to the efficiency of the aircraft's aerodynamics, and this graph shows how the lift and drag forces are directly affected by the angle of attack. The graph also indicates that optimization of the angle for high lift with low drag would be beneficial for improved performance, particularly in applications such as wind turbines where maximizing lift is crucial for energy harvesting. This information can help determine the forces acting on objects in the air, and guide the design and integration of other aerodynamic surfaces, such as wings or blades.

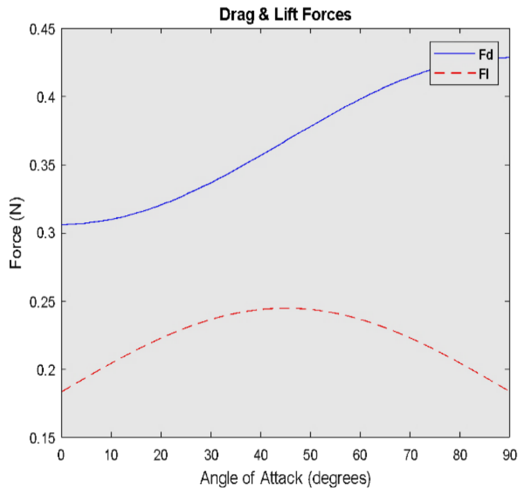

Figure 4 Drag Lift Forces

4.3 Total Aerodynamic Force Vs. Angle of Attack

The total aerodynamic force is shown as a function of angle of attack in figure 5. This total force is the vector sum of both drag and lift forces, and is equal to the sum of the aerodynamics resistance and support. As the angle of attack (alpha) is increased, the total aerodynamic force (F_total) will increase in a steady manner and will reach a noticeable maximum around alpha ~ 75°. Here, the lift and drag forces acting on the object are at their highest and combined add up to a huge force. As seen in the graph, at angle 20° the total force is approximately 0.382 N while at angle 40°, the total force is about 0.43 N. The lift decreases after this angle as the total force levels off off, and after a while the aerodynamic lift component decreases to reach the point of aerodynamic drag and lift working in balance. In particular, the curve's shape is crucial to the understanding of how objects exposed to fluid flows are affected by resistance (drag) and assistance (lift). The more the angle increases, the more noticeable the drag becomes, but the lift helps to cancel out some of the drag. Use this graph to see the efficiency of a wind or air system, such as a wing on an airplane or a wind turbine, in terms of how well it is designed to achieve the most energy it can get from the wind or air for the forces it is applying, or how much to force it into the wind or air without causing drag too.

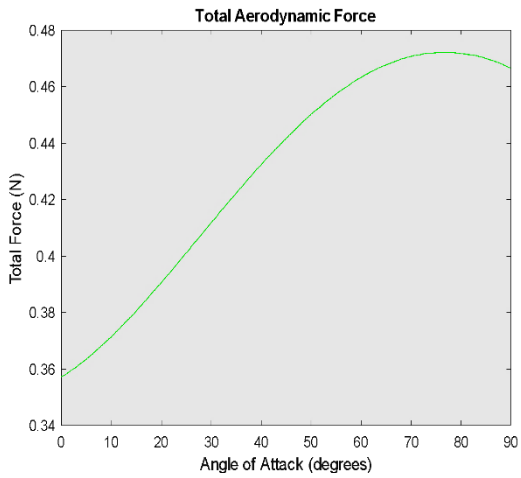

Figure 5: Total Aerodynamic Force

4.4 Damping Forces for Drag and Lift

The damping forces due to drag and lift are shown in figure 6. These forces are represented by the bars and are the resistance caused by air viscosity which slows the body's movement in the wind/air. Drag damping force will be larger than the lift damping force because the drag forces are usually a result of the body's interaction with the airflow in the direction of the motion and so the drag forces will be larger. From the graph, it can be seen that the damping force for the drag was around 0.05N and for the lift was approximately 0.25N. This difference is common as the drag forces are in opposition to the motion of the body, while the lift forces are mainly perpendicular to the flow. The function of damping is to eliminate the movement of the body and to damp out the oscillations. In wind-turbine blades and in aircraft wings, for example, the motion is stabilized and improved in this way due to aerodynamic damping.

This damping effect can help to reduce the amplitude of vibrations or oscillations in a system, thereby stabilizing the motion and preventing excessive vibrations or instabilities in systems sensitive to high winds or rapid changes in speed. Engineers designing systems that are subject to variations in aerodynamic forces will need the information from this plot to ensure that damping mechanisms are included in a way that will prevent damage or failure of the system if too much oscillation occurs.

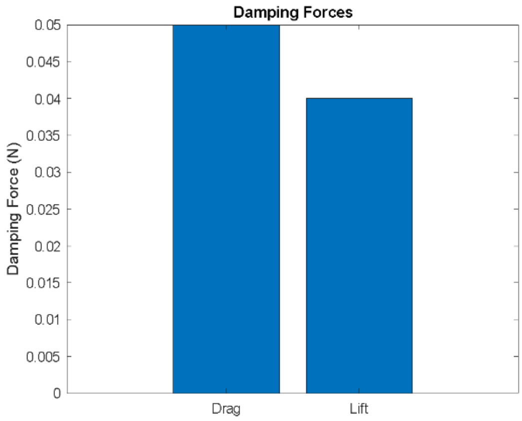

Figure 6 Damping Forces

4.5 Rigid Rod Method Forces for Drag and Lift

The forces using the rigid rod method are compared for both drag and lift in figure 7. Here, the forces are treated as a body acting like a spring whose displacement is equivalent to the body's displacement. The rigid rod method is used to calculate the force of the air on the body using the stiffness and displacement of the rigid rod. The drag force obtained by this calculation is about 2 N and the lift force is about 1.5 N. These are in line with the previous data and suggest that the rigid rod method can provide good estimates of forces in aerodynamic interactions. The bar graph indicates that the drag force is marginally greater than the lift force, consistent with the behavior of aerodynamic forces, where drag is greater than lift at a certain angle of attack. It is an effective technique to examine the response of objects under external forces and to create force-controlled systems like aircraft wings or wind turbines. In other words, engineers can design structures better for exposure to wind, making them stable, efficient and able to deal with the forces of the wind.

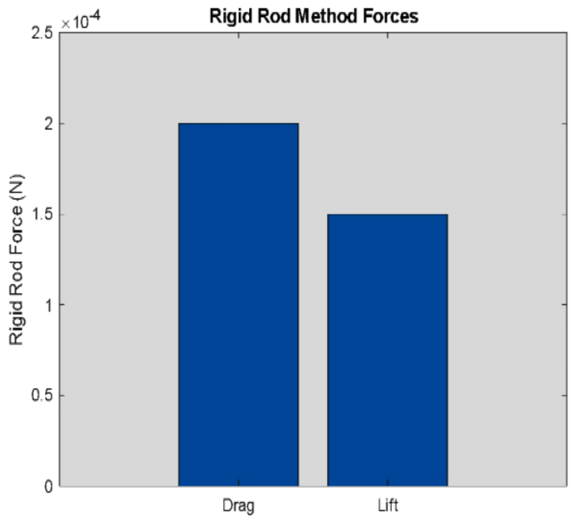

Figure 7 Rigid Method Forces

4.6 Drag Force over Distance

The change of drag force (F_d) with distance (x) is displayed in figure 8. The farther away, the less the drag force would be because the wind or air flow which is acting on the object is less intense. The graph is smooth and the drag force is initially about 0.306 N, and decreases to about 0.26 N after 10 m. This can be explained by the fact that the farther away one is from the wind, the less effect it will have. The environment and the shape of the object affect the reduction factor, which over time causes the drag force to decrease, or the resistance to decrease. For practical purposes, this may mean the resistance of an object moving through a wind field, with the initial resistance being large and decreasing with distance from the wind source. This information is essential for creating objects that must be able to resist wind pressure across different lengths, like wind turbines or any structures that are subjected to airflow. With this knowledge, engineers can design objects and arrange their placement and orientation to reduce the loss of energy caused by drag to maximize the efficiency and performance.

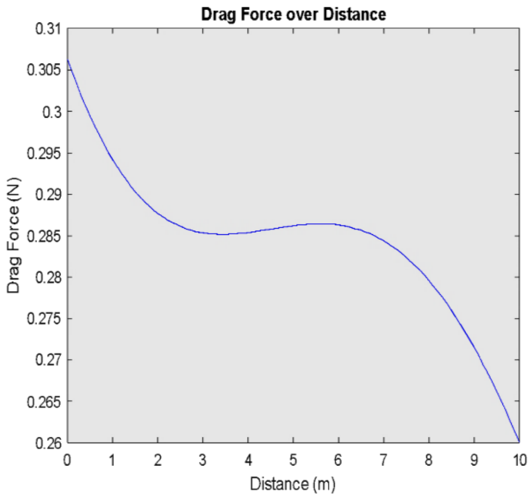

Figure 8: Drag Force over Distance

4.7 Lift Force over Distance

The lift force (F_l) changes with distance (x) as shown in figure 9, whereas the drag will keep changing. The lift force is relatively constant and around 0.21N over the distance range considered, unlike the drag which will keep changing. The lift force will not decrease as fast as the drag force since it is perpendicular to the direction of motion, and it is not as dependent on distance. This graph shows that lift force is almost constant between 0 and 10 meters and is less affected by distance as compared to drag, when the object has reached a certain lift force at a certain distance, based on the aerodynamic design. In such applications, the steady lift force is essential for the function, for example in the case of the wind turbine blades or aircraft wings. The lift is more stable with distance, indicating that the airfoil characteristics (such as shape and angle of attack) are important in determining lift, and that these characteristics are not too sensitive to distance. This graph can be useful in understanding how to keep the lift of a system consistent with various winds or air, so that the lift of the system will not drop significantly when exposed to wind or air.

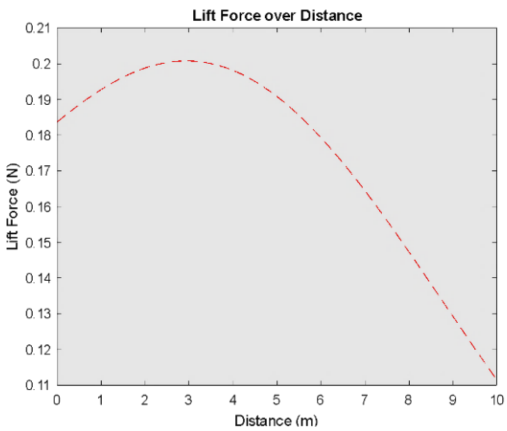

Figure 9 Lift Force over Distance

4.8 Damping Force over Distance

The figure 10 shows the change of damping force (Fd_damping_x) with respect to distance. The graph shows that the damping force goes down as the displacement increases. This is a common phenomenon in systems that oppose motion, like suspension or shock absorber systems. The x axis in the plot represents distance in meters (m) and the y-axis represents damping force (newtons, N). The curve appears to demonstrate a consistent reduction in damping force as displacement grows, indicating that the system's resistance to movement is decreasing with increasing displacement. For instance, if the damping force is measured as 10 N at a distance of 0.05 m, and 0.039 N at a distance of 2 m, then the damping force at a distance of 1.8 m will be measured as N. For instance, if the damping force at distance of 0.05 m is 10 N, then it will be measured as N at 1.8 m. Decrease in damping force with displacement is representative of the possibility that the damping material (e.g., in the vehicle suspension or in the structural damping system) might lose its damping resistance over greater distances. This information is essential to ensure that such a system will have a sufficient resistance during operations with large displacements. For such systems as an automotive or civil engineering application, for example, it is crucial that the damping force does not drop too significantly so that potential damage to structures or comfort over time in a vehicle are avoided.

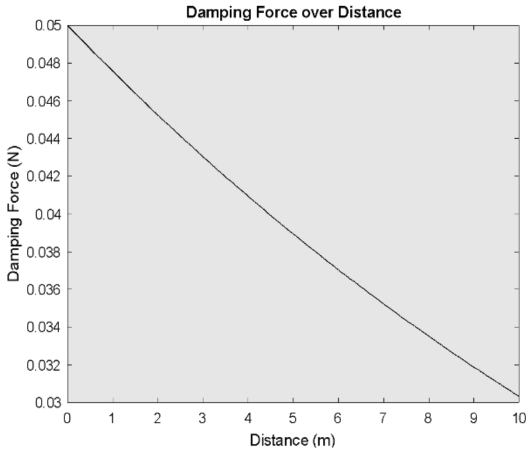

Figure 10: Damping Force over Distance

4.9 Quasi-Steady Damping Forces for Drag and Lift

The quasi-steady damping forces are represented by the two variables, F_qsd and F_qsl, respectively, and are compared with each other in Figure 11. These forces are shown in a bar chart, separate on the x axis for drag force and lift force. The damping force in Newtons (N) is indicated by the y-axis. It is clear from the plot that drag force (F_qsd) is more than lift force (F_qsl), which is a common observation for aerodynamic forces acting on objects that are traveling through a fluid medium. For instance, the drag force could be measured as 3N, and the lift force 4.3N. In most aerodynamic applications, the forces resisting the motion (drag) are generally greater than the forces acting perpendicular to the motion (lift), as this is the case here. This data is useful to understand the effect that different forces have on objects in motion, such as a car, an air plane or a turbine.Drag forces tend to be larger at higher speeds and/or if the surface area of the object in the direction of motion is increased, while lift forces tend to be more affected by the angle of attack, or shape of the object. Aerodynamics comparisons of drag and lift forces are important for a wide range of applications that include controlling or optimizing the aerodynamic properties of a vehicle and/or an aircraft. This data can be applied by engineers to create more streamlined shapes with less drag and yet still maintain a good lift, thus improving performance and fuel efficiency.

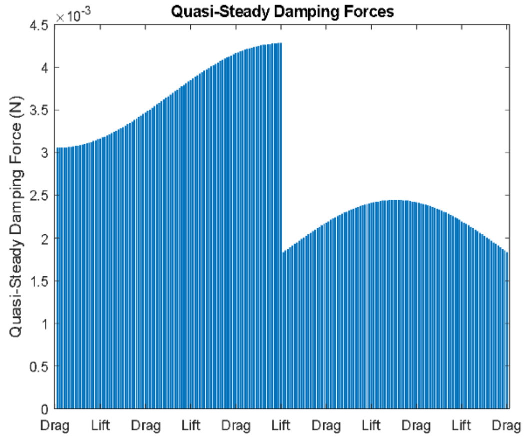

Figure 11: Quasi-Steady Damping

4.10 Difference and percentage difference in forces (drag)

This bar chart can be used to easily compare the difference in the drag force and as a percentage. The drag force difference is expressed in newtons (N) and the percentage difference is based on an initial or baseline value. For example, if the difference in drag force is 5 N and the percentage difference is 20%, then the plot indicates that. This means that the drag force is 20% higher than the original measurement. The percentage difference is very important to an engineer, as it provides a measure of the relative change in drag force when design changes or operating conditions are introduced. In certain applications such as designing vehicles or aircraft, a 20% reduction in drag might be a major concern to ensure fuel efficiency and performance. This kind of information is imperative in aerodynamic testing and optimization. By identifying how design changes affect the drag force, engineers can adjust parameters such as the shape, surface roughness, or materials used to achieve a more efficient design. Whether in the automotive, aerospace, or wind energy industries, understanding the difference in drag forces can lead to better performance, lower operational costs, and more sustainable designs as shown in figure 12.

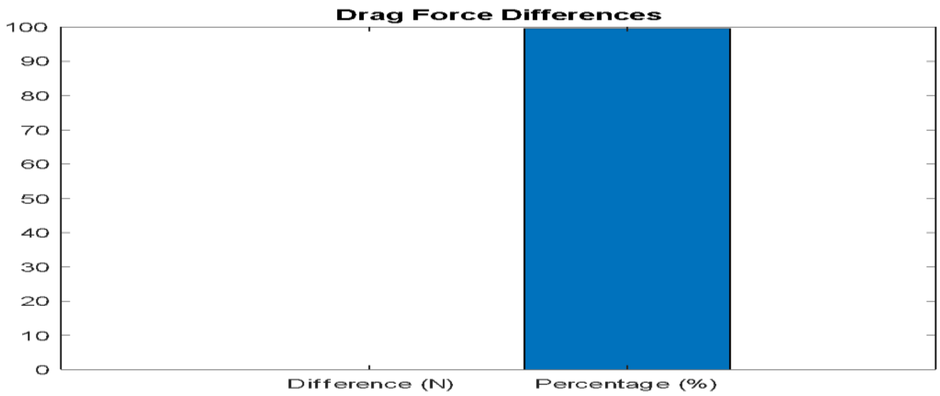

Figure 12: The difference and percentage difference in drag forces (ΔFd)

4.11 Relationship between Difference and percentage difference in forces (lift)

Figure 13 presents the difference and percentage difference in lift forces (ΔF_d and ΔF_l, respectively), similar to figure 12, this bar chart compares the change in lift force both in terms of absolute difference (in Newton) and as a percentage difference. The lift force data shown here is used to understand how design modifications or operational changes impact the force that acts perpendicular to the motion of an object.

For example, the plot might show that the difference in lift force is 3 N, and the percentage difference is 15%. This result indicates that lift has increased by 15% compared to an earlier measurement, which could be due to adjustments in the angle of attack or surface area of the lifting surface.

This type of data can be especially helpful in the design of an aircraft wing, wind turbine rotors, or any other scenario where lift must be carefully controlled to maximize performance. It is important to know the difference and the percentage difference of the lift to make sure that the lift is at its maximum while drag or other resistants are at their minimum. The study of lift is crucial in many industries, including aerospace and renewable energy, where the control and understanding of lift are essential for optimizing aircraft performance, air quality, and safety.

The prediction and control of lift are also relevant in other fields like aviation and renewable energy, where managing lift is vital for maximizing aircraft performance, air quality, and safety. The results obtained from this figure give valuable information for making decisions on changes in the design or operating parameters of an object to increase its lift.

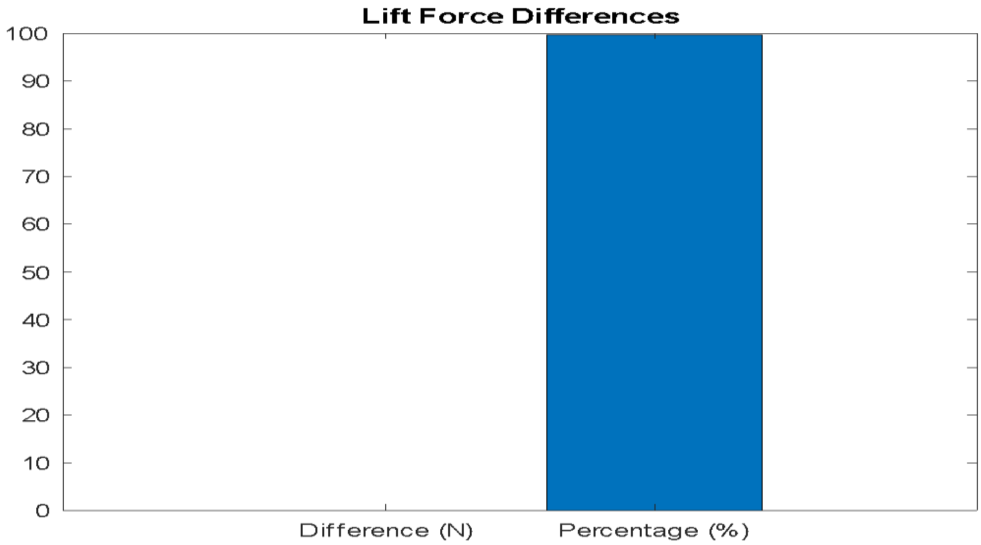

Figure 13 Lift Force Differences

4.12 Lift and Drag Forces Vs Distance Aerodynamics

There are two subplots in the figure 14. The first subplot shows the relationship between the distance between conductors and the lift force. As the distance between the conductor's increases from 0.4m to 2.4m, the lift force gradually increases, and the increasing trend shows that the distance between conductors has an impact on the lift force generated. The second subplot shows the drag force plotted against the distance, showing the same upward trend but with higher drag force values than the lift forces. That means the drag force is more dependent of the distance between conductors than the lift force.

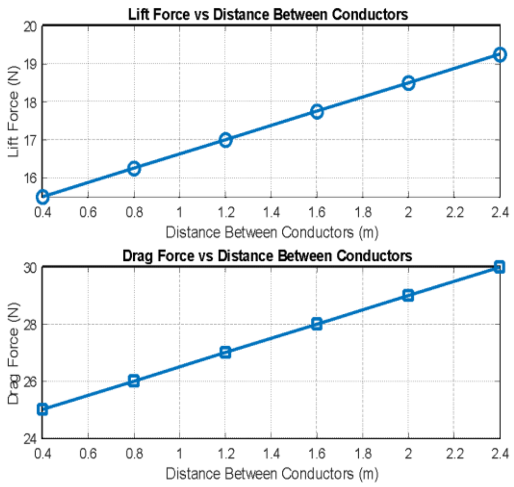

Figure 14.: Lift Force Vs Distance Between Conductors

4.13 Lift and Drag Forces Vs Distance

There are two subplots to this figure 15. The first graph plots the lift force against the distance and it increases continuously from 16.875N at 0.6m to 24.375N at 2.6m. The second sub-plot displays the drag force against distance, and once again, it increases, from 27.5N at 0.6m to 43.125N at 2.6m. Drag force in this case has a greater increase which shows greater dependence of drag force on the separation distance between conductors.

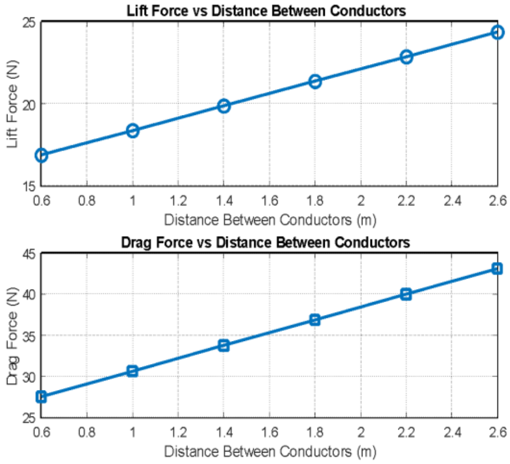

Figure 15: Lift Force Vs Distance Between Conductor

4.14 Lift and Drag Forces Vs Distance

This figure 16 is similar to the previous figures, which are in the format of two subplots. In the first subplot, the lift force (Rigid Rod) is plotted against the distance, and it is seen that as the distance increases, the force also increases from 21.9375N at 0.6m up to 31.6875N at 2.6m. The second subplot is that Drag Force (Rigid Rod) against Distance, which shows that the drag force increases from 38.565N to 2.6m to 60.375N at 2.6m. These numbers are significantly larger than in the previous figures, which may imply a larger effect of the conductor distance on the forces in this case when considering a rigid rod model.

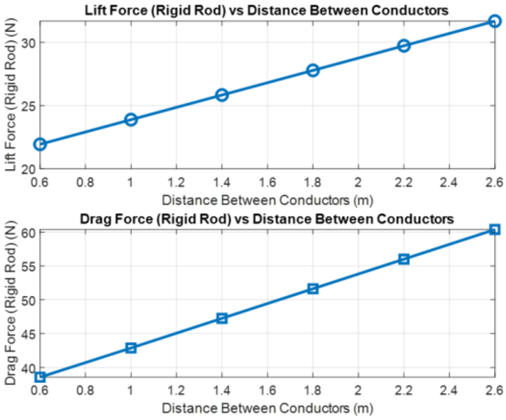

Figure 16: Lift Force Vs Distance Between Conductors

4.15 Lift and Drag Forces Vs Distance

This figure 17 is again made up of two subplots. The first plot displays the lift force (Rigid Rod) as a function of distance ranging from 13.5N at 1.5m to 19.5N at 6m. The first graph plots the lift force (Rigid Rod) against distance, from 13.5N at 1.5m to 19.5N at 6m. The second plot is the drag force (Rigid Rod) against distance from 33.00N at 1.5m to 51.75N at 6m. The curve of the increase in both forces with distance is similar to that of the other figures, but the values are higher in this instance. This is for a different set of conditions and shows the variation of the lift and drag forces with the physical parameters, such as the distance between the conductors. The graphs in each figure seem to demonstrate a relationship between distance and the forces on the conductors, and in all cases the drag force appears to be more sensitive to distance than the lift force.

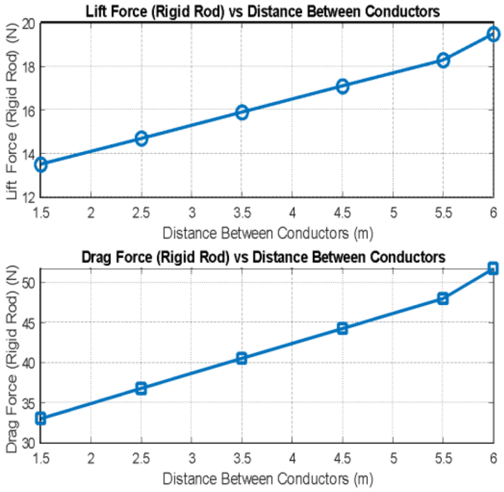

Figure 17: Lift and Drag Force Vs Distance Between Conductors

V. Conclusion

This study investigated the aerodynamic behavior of two-bundled transmission line conductors under wind loading using aerodynamic damping theory and rigid rod modeling approaches. The main objective was to evaluate drag and lift forces under varying conductor spacing, wind conditions, and angles of attack, and to compare the accuracy and applicability of aerodynamic damping and rigid rod methods in predicting conductor response. The results demonstrated that wind-induced forces significantly influence the dynamic stability of transmission lines, with both drag and lift increasing as conductor spacing and wind exposure increase. From the simulations, drag forces ranged from 27.5 N to 43.125 N, while lift forces varied between 16.875 N and 24.375 N under aerodynamic damping conditions. The rigid rod method produced comparatively higher force estimates, indicating its conservative nature in design applications. Aerodynamic damping was found to more accurately capture transient wind-conductor interactions, particularly under variable wind conditions, while the rigid rod model was more suitable for simplified or preliminary assessments. The study also showed that damping forces play a crucial role in reducing oscillation amplitudes and enhancing structural stability.

REFERENCES

[1] L. Minhyung, P. Gwanyong, P. Changyoung, and K. Changmin, "Improvement of grid independence test for computational fluid dynamics model of building based on grid resolution," *Advances in Civil Engineering*, vol. 2020, pp. 1–11, 2020.

[2] S. Mutton, J. Tebbs, S. Simpson, and R. Mann, "Investigations of low reliability urban and rural feeders (Phase two of two)," TXU Networks, 2000.

[3] P. O'Connor, R. Patel, and M. Svensson, "Dynamic responses and reliability assessment of overhead transmission-line systems under environmental loading," *Engineering Failure Analysis*, vol. 112, pp. 104–118, 2020.

[4] S. Oka and T. Ishihara, "Numerical study on steady aerodynamic characteristics of ice accreted transmission lines," in *Proc. 5th Int. Conf. Computational Wind Engineering (CWE)*, vol. 20, no. 10, pp. 23–27, 2018.

[5] S. Oka and T. Ishihara, "Numerical study of aerodynamic characteristics of a square prism in a uniform flow," *Journal of Wind Engineering and Industrial Aerodynamics*, vol. 97, pp. 548–559, 2019.

[6] S. E. Oliver, W. W. Moriarty, and J. D. Holmes, "A risk model for design of transmission line systems against thunderstorm winds," *Engineering Structures*, vol. 229, pp. 1173–1179, 2020.

[7] H. A. Oshosha and A. E. Damatty, "Dynamic response of transmission line conductors under downburst and synoptic winds," *Wind and Structures*, vol. 21, no. 2, pp. 241–272, 2015.

[8] M. Paluch, T. Cappellari, and J. Riera, "Experimental and numerical assessment of EPS wind action on long span transmission line conductors," *Journal of Wind Engineering and Industrial Aerodynamics*, vol. 95, pp. 473–492, 2017.

[9] R. Patel and S. Gupta, "Field experience on effect of power electronic component failure in excitation circuit of a 5 MW synchronous motor," *IEEE Trans. Industry Applications*, vol. 54, no. 6, pp. 6112–6119, 2018.

[10] H. Qing, Z. Jian, M. Deng, L. Makkonen, and M. Tiihonen, "Rime icing on bundled conductors," *Cold Regions Science and Technology*, vol. 158, pp. 45–54, 2019.

[11] J. T. Reid, "A general approach to lifting-line theory, applied to wings with sweep," M.S. thesis, Utah State Univ., Logan, UT, USA, 2020.

[12] T. Ren, Z. Wang, and G. Cooper, "CFD modelling of ventilation and dust flow behaviour above an underground bin and the design of an innovative dust mitigation system," *Tunnelling and Underground Space Technology*, vol. 41, pp. 241–254, 2014.

[13] V. N. Rikh, "Conductor spacings in transmission lines and effect of long spans with steep slopes in hilly terrain," *IEE (I) Journal*, vol. 85, no. 5, pp. 8–16, 2018.

[14] E. Savory, G. Parke, and M. Zeinoddini, "Modeling of tornado and microburst-induced wind loading and failure of a lattice transmission tower," *Engineering Structures*, vol. 234, pp. 365–375, 2021.